Molecular Modeling of a Tandem Two Pore Domain Potassium Channel Reveals a Putative Binding Site for General Anesthetics

Edward J. Bertaccini,*[†,§] Robert Dickinson,[∥] James R. Trudell,[†,‡] and Nicholas P. Franks[⊥]

[†]Department of Anesthesia, [‡]Beckman Center for Molecular and Genetic Medicine, Stanford University School of Medicine, Stanford, California 94305, United States

[§]Department of Anesthesia and Perioperative Medicine, Palo Alto VA Health Care System, Palo Alto, California 94304, United States

[∥]Department of Surgery & Cancer and [⊥]Department of Life Sciences, Imperial College, London SW7 2AZ, United Kingdom

S Supporting Information

ABSTRACT: Anesthetics are thought to mediate a portion of their activity via binding to and modulation of potassium channels. In particular, tandem pore potassium channels (K2P) are transmembrane ion channels whose current is modulated by the presence of general anesthetics and whose genetic absence has been shown to confer a level of anesthetic resistance. While the exact molecular structure of all K2P forms remains unknown, significant progress has been made toward understanding their structure and interactions with anesthetics via the methods of molecular modeling, coupled with the recently released higher resolution structures of homologous potassium channels to act as templates. Such models reveal the convergence of amino acid regions that are known to modulate anesthetic activity onto a common three- dimensional cavity that forms a putative anesthetic binding site. The model successfully predicts additional important residues that are also involved in the putative binding site as validated by the results of suggested experimental mutations. Such a model can now be used to further predict other amino acid residues that may be intimately involved in the target-based structure—activity relationships that are necessary for anesthetic binding.

KEYWORDS: Tandem pore potassium channel, anesthesia, homology modeling
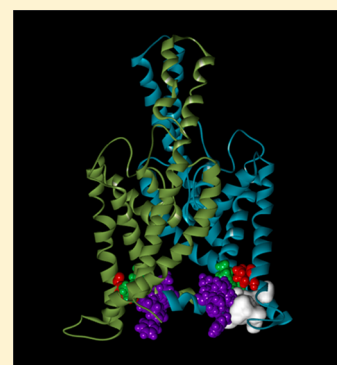
Volatile general anesthetics are thought to act, at least in part, by binding to and modulating two pore domain potassium channels (K2P). These K2P potassium channels are transmembrane ion channels whose current is modulated by the presence of a wide range of volatile and gaseous general anesthetics,[1−3] and whose genetic knock out, either globally[4−6] or locally,[7] has been shown to confer a level of anesthetic resistance. What is not known is where anesthetics bind within the channels, and how this binding translates into increased channel opening. For different K2P channels, using a combination of chimeric constructs and site-directed mutagenesis, a number of amino acids have been identified as key anesthetic determinants.[8−11] However, whether these determinants function as parts of anesthetic binding sites or are involved in transduction mechanisms that convert binding into channel gating is unclear. The covalent modification work by Conway and Cotton suggests that a region around L159 forms a putative anesthetic binding site.[12] Another approach to this problem is to use the structures of homologous potassium channels as templates to construct models of an anesthetic-sensitive channel to investigate the three-dimensional disposition of these anesthetic determinants. Here we describe how the construction of such models reveals the convergence of amino acid regions that are known to affect anesthetic sensitivity into a common three-dimensional locus that could serve as an anesthetic binding site. We test our prediction that particular amino acids form part of an anesthetic binding site

using patch-clamp electrophysiology on wild-type and mutant K2P channels.

A novel anesthetic-activated potassium current was first characterized in a single molluscan neuron by Franks and Lieb.[13,14] Following this, anesthetic activated mammalian K2P channels were identified and knockout mice lacking K2P channels have demonstrated decreased sensitivities to volatile anesthetics.[2] Within the tandem pore potassium channel family, TREK-1 is sensitive to the anesthetic gases Xe, N_2O, and cyclopropane, while TASK-3 is insensitive to these gases while retaining sensitivity to the volatile anesthetics.[9] Additional studies producing single point mutations in TREK-1 conferred relative resistance to certain volatile anesthetics.[8] Through the generation of TASK-3 knockout mice, Pang et al. showed a significant role for the TASK-3 potassium channel in the theta oscillations of the cortical EEG that are associated with both sleep and anesthetized states.[6] In particular, TASK-3 knockout animals show marked alterations in both anesthetic sensitivity and natural sleep behavior. This is particularly tantalizing, since certain electrophysiologic aspects of deep (non-REM) sleep have similarities to the anesthetized state.[15,16]
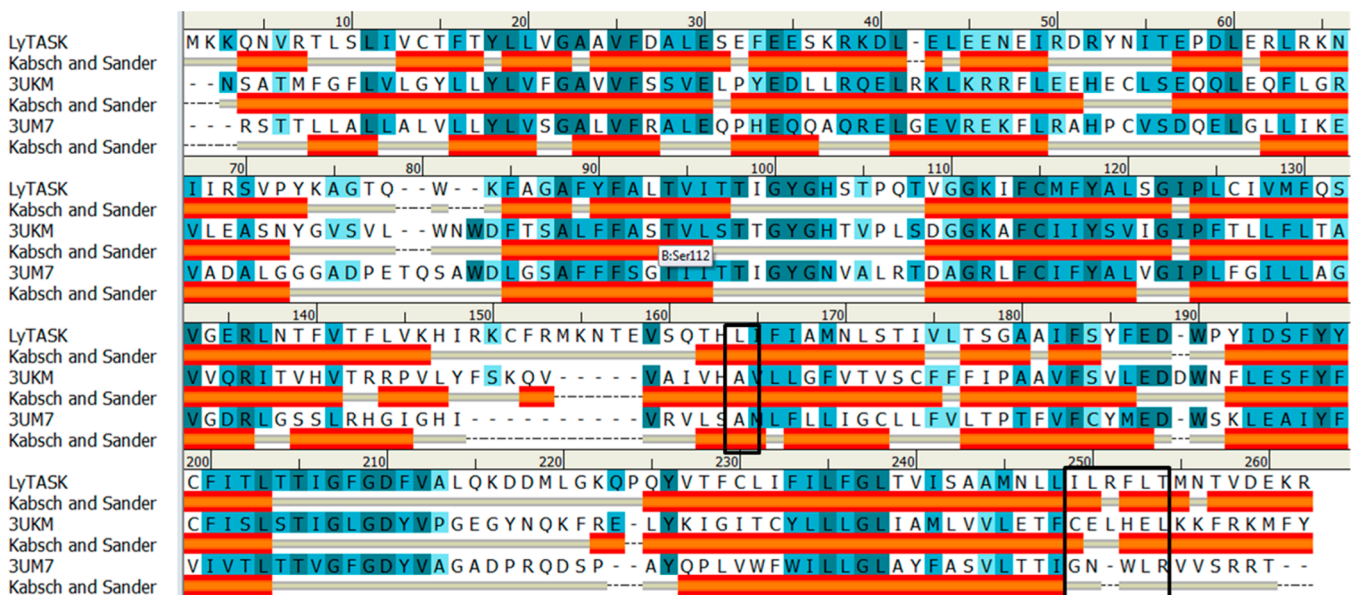
Figure 1. Multiple sequence alignment of the two templates with LyTASK. L159 and the ILRFLT sequences are outlined in boxes. Note the differences in the aligned amino acids between LyTASK and 3UKM/TWIK (both anesthetic sensitive) and 3UM7/TRAAK which is anesthetic insensitive. Amino acid similarity is denoted by shades of blue, with darker indicating greater similarity. Note also the alpha helical structure identified by the Kabsh and Sander algorithm for each structure indicated by the orange bars.

RESULTS

Molecular Modeling. We chose to model the TASK potassium channel from *Lymnaea stagnalis* (LyTASK), because this has the greatest sensitivity to volatile anesthetics of any known K2P channel.[8] The BLAST-derived scores suggest a close homology between LyTASK and two K2P channels whose structures have been determined to high resolution. The first is the anesthetic-sensitive human TWIK-1 channel, 3UKM[17] (51% sequence coverage, 33% maximum amino acid identity, and BLAST expectation value of 4×10^{-29}), and the second is the human anesthetic-insensitive TRAAK channel, whose structure has been described with two different chain connectivities 3UM7 and 4I9W[18,19] (67% sequence coverage, 31% maximum amino acid identity, and BLAST expectation value of 3×10^{-31}). Subsequent CLUSTALW alignment of the sequence from LyTASK to the sequence profile (created from the sequences of the two templates 3UKM and 3UM7) also demonstrates reasonable sequence similarity (Figure 1). Models of the anesthetic-sensitive LyTASK based on the overlapped TWIK-1 and TRAAK template structures show a dimer with symmetry about a central ion pore. Amino acid regions notable for modulating anesthetic action on this channel (L159[8] and the amino acid sequence ILRFLT[10,11]) converged on a common pocket in three-dimensional space (Figure 2). This was the case even in a model with the alternative backbone connectivities based on 4I9W, though the latter was not used for further analysis. The different connectivity only affected regions that are at the opposite end of the channel to the putative anesthetic binding site and therefore is unlikely to impact on our results or conclusions. Three-dimensional visualization of our model suggested that L241, L242, and S155 were adjacent to the critical residues (L159 and the sequence ILRFLT) that have previously been demonstrated as having large effects on anesthetic modulation.[8,10,11] Additionally, the model suggests that the L159 might form part of an interacalated hydrophobic side chain interaction with L241 and L242 (see Figures 3 and 4) as well as
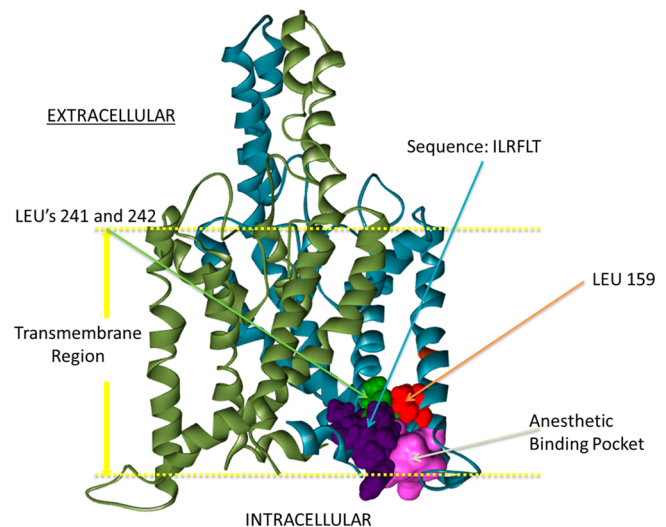

Figure 2. Molecular modeling derived from the consensus overlap of templates reveals a putative general anesthetic binding site. Model of LyTASK illustrating the positions of two established determinants of anesthetic sensitivity: L159 and the critical sequence of ILRFLT amino acids.[8,10,11] The putative anesthetic binding pocket is shown by the pink surface, but its intracellular extent is rather arbitrary due to its "cave-like" opening in that direction.

demonstrating residue proximities that could allow a possible polar interaction between S155 and R246 (Figure 3). The disruption of such interactions between alpha helical secondary structure units could lead to changes in the tertiary structure as well as the large scale motions of the protein.

Electrophysiology on Wild-Type and Mutant LyTASK Channels. Cells transfected with wild-type LyTASK cDNA exhibited robust outwardly rectifying currents that reversed close to the calculated potassium reversal potential (Figure 5A, blue line; Figure 5B—F, solid lines). Halothane (3%) resulted in activation of both wild-type and mutant LyTASK currents
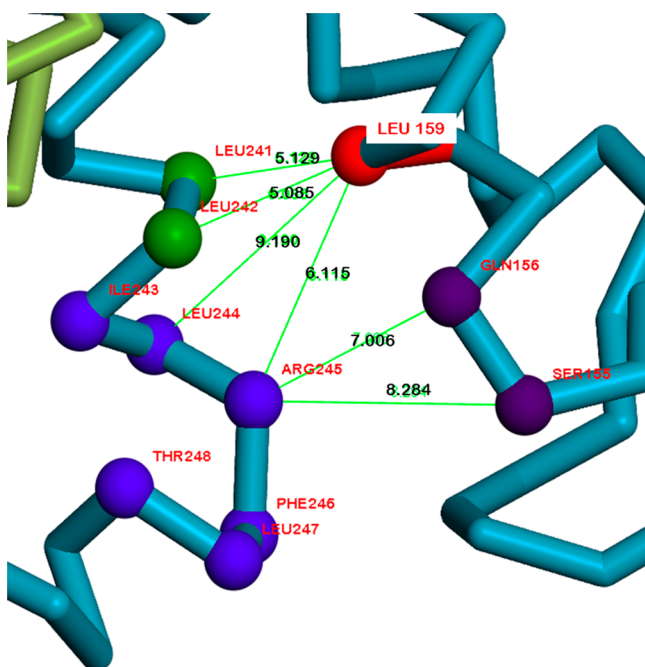
Figure 3. Model of LyTASK derived from the consensus overlap of templates illustrating the position of L159 relative to other adjacent residues for possible mutational analyses. In particular, note the positions of L241 and L242. Distances between respective α carbon atoms are expressed in angstroms. Also notice the distances from R245 to both S155 and Q156 for possible polar interactions.
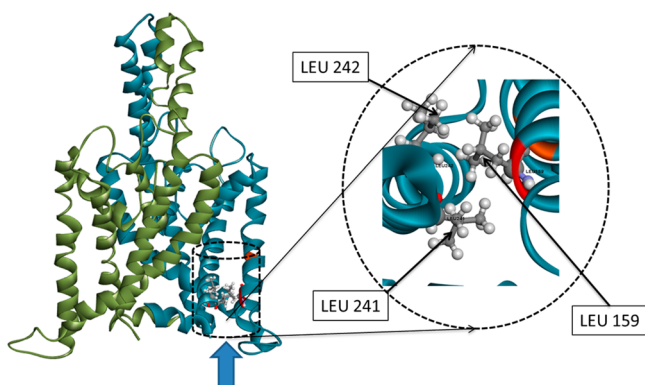
Figure 4. Expanded view (cylinder rotated 90°) of a possible anesthetic binding region, as viewed from the intracellular surface (blue arrow), illustrating the side chain intercalation of LEU 241 and 242 from one α helix with LEU 159 of the adjacent α helix.

(Figure 5A, red line; Figure 5B−F, dashed lines). The mean wild-type current, measured at −50 mV, was 448 ± 112 pA (Figure 6A, Table 1). Mutation of serine 155 to alanine, or lysine 242 to alanine, had little effect on the control LyTASK current in the absence of halothane (Figure 6A, Table 1)). Mutation of serine 155 to tryptophan or lysine 241 to alanine caused reductions in the LyTASK currents (Figure 6A, Table 1); these reductions were not significant compared to wild-type (Figure 6A, Table 1), but in the case of the S155W mutant there was a trend toward significance ($p = 0.06$). In both wild-type and mutant LyTASK channels, halothane (3%) activated the LyTASK current, but the degree of activation was different (Figure 6B). This was most notable when the degree of activation was expressed as a percentage of the baseline LyTask current in the absence of anesthetic. Halothane (3%) activated

the wild-type LyTASK currents by 412 ± 54% (Figure 6C). The LyTASK L241A and the L242A mutants showed a significantly reduced activation by 3% halothane compared to the wild-type channel, with 190 ± 11% and 194 ± 14% activation, respectively (Figure 6C). To test a hypothesized polar interaction between S155 and R246, we mutated LyTASK S155 to an alanine. The effect of 3% halothane on this S155A mutant showed no significant difference compared to wild-type (393 ± 62% activation). We also mutated S155 to a bulky aromatic residue, tryptophan, to see if this might mimic the presence of an anesthetic in our putative binding pocket. The S155W mutant showed a marked increase in activation by 3% halothane, with the 1146 ± 20% activation being ∼2.8 times that of the effect of halothane on the wild-type channel (Figure 6C and Table 1).

DISCUSSION

General anesthetics have been employed for over 165 years, and their use is indispensible in a variety of invasive surgical procedures and an ever increasing body of screening and preventive medicine maneuvers (colonoscopy, bronchoscopy, etc.). The state of general anesthesia is characterized by profound lack of awareness, plus amnesia, analgesia, and immobility. Each of these desirable physiological responses is likely to be a consequence of anesthetic effects on different parts of the central nervous system, and considerable progress has been made toward identifying these sites.[20−22] At the cellular level, it appears that anesthetics act predominantly at a relatively small number of molecular targets, in particular, GABA_A receptors, two-pore domain potassium channels, and NMDA receptors.[21] In order to further pinpoint molecular sites of anesthetic action, a large number of in vitro site-directed mutagenesis studies have been performed, identifying particular amino acids and motifs that are required for the effects of both volatile and intravenous general anesthetics on a wide variety of ion channels.[20−22] Effects have been catalogued across different ion channel proteins without convergence on a single site of action. Another approach to identify relevant receptors has involved the genetic modification of whole organisms in an effort to induce resistance to particular anesthetics and to test the importance of a putative target. To date, two key molecular targets have emerged from this combination of in vitro and in vivo approaches: the GABA_A receptor and K2P potassium channels. The N265 M knock-in mutation in the mouse β3 GABA_A receptor subunit[23] conferred increased resistance to both propofol and etomidate for both loss of righting reflex (a rodent surrogate for loss of consciousness in humans) and loss of response to a painful stimulus. While a great deal of work has focused on the modeling of anesthetic binding sites within the GABA_A receptor,[24,25] several studies have shown that this class of proteins is unlikely to mediate all of the effects of anesthetics, particularly for the volatile agents. It is also likely that anesthetics act by binding to and modulating K2P potassium channels.[21] The knockout of two different tandem pore potassium channels[4−7] conferred enhanced resistance to volatile general anesthetics.

In this Article, we now show how molecular modeling can be used to shed light on molecular mechanisms of anesthetic action as well as more efficiently suggest in vitro mutations for testing of molecular models. In this case, molecular modeling allows one to leverage the knowledge that is gleaned from the recently available high-resolution crystallographic coordinates for K2P potassium channels that are highly homologous to one
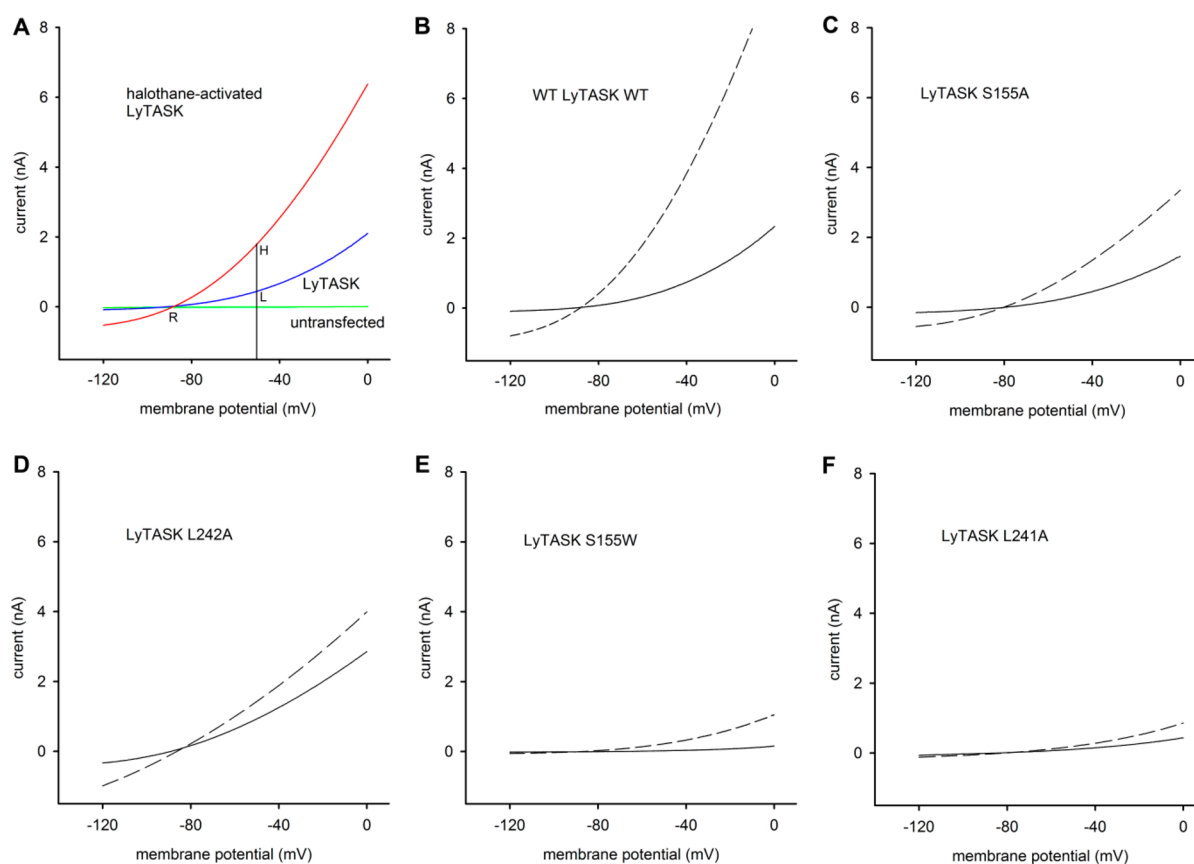
Figure 5. Typical electrophysiology current−voltage relations for the WT and mutant LyTASK potassium channels. (A) Schematic diagram showing current−voltage relation for an untransfected cell (green line), LyTASK transfected cells exhibit a large outwardly rectifying potassium current (blue line) reversing close to −90 mV (R). In the presence of halothane (red line), the LyTASK current is increased. LyTASK currents are quantified by measuring the value of the current at a membrane potential of −50 mV, marked on the diagram is the control LyTASK current "L" and the halothane-activated LyTASK current, "H". (B) Wild-type LyTASK. (C) LyTASK S155A mutant. (D) LyTASK L242A mutant. (E) LyTASK S155W mutant. (F) LyTASK L241A mutant. Solid lines are LyTASK currents in the absence of halothane, and dashed lines are the LyTASK currents in the presence of 3% halothane. Data were sampled at 20 kHz, and each trace contains 3000 data points. Lines shown are means of 10 individual voltage ramps for a given cell in each condition.

that has been extensively studied by mutagenesis and electrophysiologic analyses. Mutations at L241 and L242 may blunt activation by anesthetics possibly through a disruption of a intercalated hydrophobic side chain interactions (Figure 4). However, the mutations at S155 seem to only have an effect of potentiating anesthetic activation when the substituted side chains are large enough, possibly simulating the presence of ligand. Initial predictions on the importance of a partial polar interaction between S155 and R246 seem disproven by the fact that there is no effect on anesthetic activation when the polar to nonpolar S155A mutation is introduced. The greater potentiation by the S155W mutation may indicate that a larger than normal side chain protruding into an anesthetic binding site accentuates an effect resulting from anesthetic binding, especially with the tryptophan side chain being significantly larger than a single halothane molecule. One could postulate that such an effect may indicate that the anesthetic binding site in LyTASK could accommodate two halothane molecules, as has been previously shown on anesthetic binding to cholesterol oxidase[26] and firefly luciferase.[27,28]

Certain caveats should be noted in regards to interpretations from our modeling. The templates upon which the homology modeling are based are of sufficient resolution to allow good side chain visualization. However, there are some residues in chain B of TRAAK that are not present in the crystal structure.

This causes Modeler to build the same loop in chain B of the LyTASK model based solely on TWIK, which is more collapsed in the direction of any binding site, causing slightly different pocket formations in this region versus that composed of template chains A. Also, the alignment of the positions in the templates that are homologous to L159 in LyTASK show reasonable homology (alanines instead of leucine). However, there is rather poor homology in the regions of the templates associated with the ILRFLT motif within LyTASK. This leaves some potential for variability in the alignments. Such alignments would require experimental validation as has been presented here.

Furthermore, at this stage, our model does not explain the differential anesthetic sensitivities of some K2P channels over others. Our unpublished preparatory work to the current study did not demonstrate any notable differences in pocket sizes between TRAAK and TWIK in these areas that would account for differential anesthetic sensitivities. However, the point of this work is to demonstrate the convergence of relevant residues on a common 3D locale that has pocket-like character allowing quite variable size accessibility from the extracellular space. Such accessibility is clearly present in both the TRAAK and TWIK templates. The differential sensitivity of these proteins is most likely due to different amino acid side chains being present in the binding pocket, as well as different large

1249

dx.doi.org/10.1021/cn500172e | ACS Chem. Neurosci. 2014, 5, 1246−1252
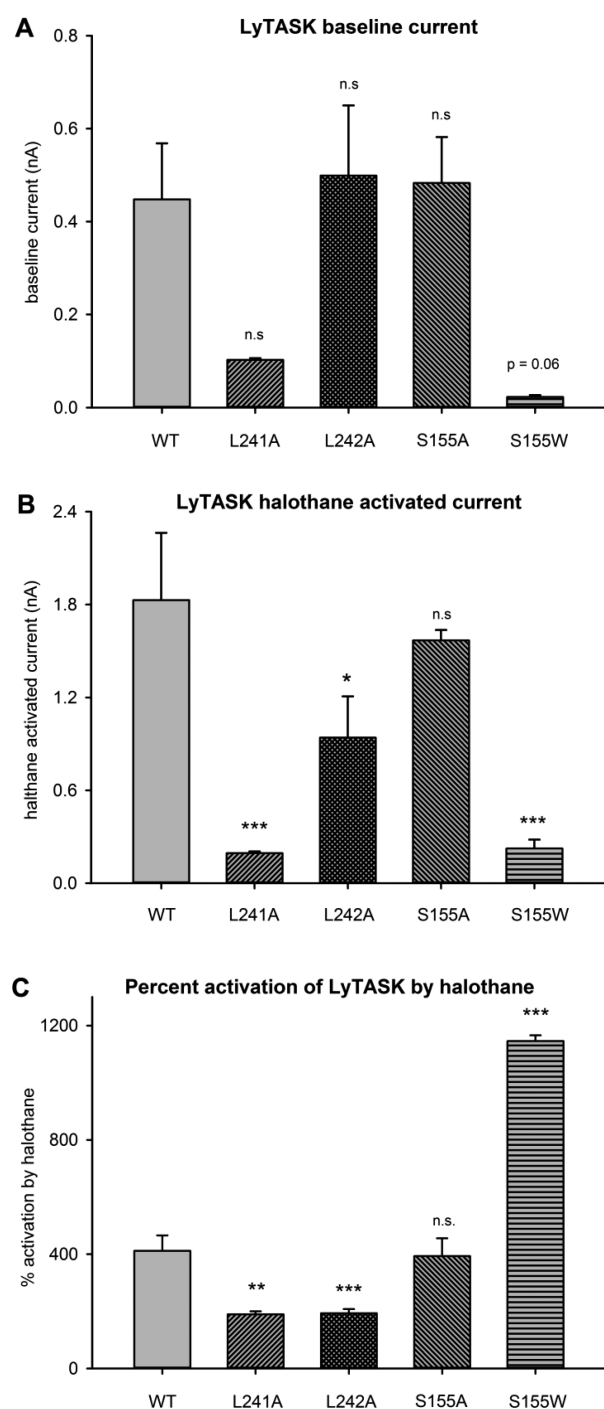
Figure 6. Effect of point mutations in LyTASK currents on (A) baseline control current at −50 mV ("L" in Figure 5A), (B) halothane activated current at −50 mV ("H" in Figure 5A), and (C) percentage activation by halothane. Percentage activation is calculated using $(H/L − 1) × 100\%$. Values shown are means, and error bars are SEM ($n = 7$ WT, $n = 4$ L241A, $n = 7$ L242A, $n = 5$ S155A, $n = 5$ S155W). ***$p < 0.001$, **$p < 0.01$, *$p < 0.05$ compared to WT; one-way ANOVA with Bonferroni's post hoc test.

scale motions that may affect binding to this site. While the global homology among templates and LyTASK can be seen in Figure 1 more clearly, the regional homology is relatively low. The latter amino acid side chain variability as well as the amphiphilic nature of the amino acids present both could contribute to differential anesthetic sensitivity. Furthermore,

Table 1. Anesthetic Activation of Wild-Type LyTASK and Mutant Channels[a]

channel genotype	percentage activation by 3% halothane	control current (L) (pA)
wild-type ($n = 7$)	412 ± 54%	448 ± 112
L241A mutant ($n = 4$)	190 ± 11%**	103 ± 4
L242A mutant ($n = 7$)	194 ± 14%***	499 ± 150
S155A mutant ($n = 5$)	393 ± 62%	483 ± 99
S155W mutant ($n = 5$)	1146 ± 20%***	23 ± 4

[a]Currents were measured at a membrane potential of −50 mV. Percentage activation was calculated from $(H/L − 1) × 100\%$. Significantly different (**$p < 0.01$; ***$p < 0.001$) from wild-type (one-way ANOVA with Bonferroni's post hoc test).

although most work on anesthetic binding to soluble proteins shows little effect on protein structure when anesthetics bind, such changes may occur in integral membrane proteins. Either way, the location of the binding pocket at the surface of K2P channels, in addition to its amphiphilic character, may lend itself to a considerable amount of ligand size promiscuity, as exemplified by the differential effects of ligands from Xe to isoflurane.

Finally, the localization of residues important for anesthetic binding may only infer a putative binding site. Another interpretation could be that such residues merely form a region which is critical for allosteric modulation of the anesthetic-mediated effect. Greater evidence for actual anesthetic binding could come from experiments involving the covalent localization of an anesthetic-like ligand to the putative anesthetic binding site. Additionally, a concern could be that the open state probability of residue-241 and -242 mutants may be near 100%. We cannot exclude the possibility that the mutations affect channel gating, but the fact that we can activate all of the mutant channels with halothane indicates that the open probability is less than 100% in all cases. In addition, Conway and Cotten have shown that LyTASK L159C and TASK3M159C, both anesthetic resistant, tolerate further activation by alkylation, implying the channels are not "locked open" by loss of leucine or methionine in this region and that acute changes in steric occupancy between residues 241, 242, and 159 activate the channel.[12]

■ CONCLUSION

Homology modeling produced a model of the K2P channel that revealed a putative anesthetic-binding pocket identified by the convergence of amino acid residues known to modulate anesthetic activity. The anesthetic binding pocket model was validated by the successful prediction of other amino acid residues also found to alter anesthetic modulation of the channel due to their spatial proximity to the putative binding site. Such a model can now be used to further predict other amino acid residues that may be intimately involved in the target-based structure−activity relationships that are necessary for anesthetic binding.

■ METHODS

Molecular Modeling. All protein construction calculations were performed in the Discovery Studio 3.5 software suite (Accelrys, San Diego, CA). The amino acid sequence of the K2P channel from the snail, *Lymnaea stagnalis* (LyTASK), was obtained from the National

Center for Biotechnology (NCBI) database. A BLAST sequence search[29] was performed using this sequence to search for sequences of high homology from those of known three-dimensional (3D) structure. The two best-scored homologous human sequences were downloaded as 3D coordinates for two forms of tandem pore potassium channels. These were obtained from the Research Collaboratory for Structural Bioinformatics (RCSB) database[30] as the human two pore domain potassium ion channels known as TWIK-1 or K2P1 (PDB code: 3UKM)[17] at 3.4 Å resolution and TRAAK or K2P4.1 (PDB code: 3UM7)[19] at 3.31 Å resolution. A multiple structure alignment was performed using the SAlign algorithm[31] to create a sequence profile based upon this structural alignment. A sequence (from LyTASK) to profile (from the SAlign templates) alignment was then performed with ClustalW[32] so as to align the sequence of the unknown structure with those of the known structures. The Modeler module[33] was used for assignment of coordinates for aligned amino acids, the construction of possible loops, and the initial refinement of amino acid side chains. Side chain refinement was performed on all residues with only one set of potassium ions present and both undecanes present after atom typing with CHARMm[34] atom types and CFF charges.[35] Molecular mechanics optimization of the entire structure was performed with free side chains in vacuo and a 10 kcal mol^{-1} Å^{-2} harmonic restraint on the α carbon protein backbone. Amino acid regions on this channel that are known to be anesthetic determinants (L159[8] and the sequence ILRFLT[11]) were mapped onto the resulting structure.

Additional molecular modeling was performed using a modified version of a more recently released template of a tandem pore potassium channel with a different amino acid backbone connectivity. The TRAAK or K2P4.1 channel (PDB code: 4I9W[18,19]) is a tandem pore potassium channel that is insensitive to anesthetics, but provides higher resolution analysis that suggests altered backbone connectivity. Even though this region of controversial connectivity is quite distant from the anesthetic binding site in question, another model of LyTASK was constructed utilizing the amino acid backbone connectivity corrected to that of 4I9W along with 3UKM as the primary template. Once again, the LyTASK sequence was aligned to this, now a mix of templates, via the ClustalW algorithm. The Modeler module was used for assignment of coordinates for aligned amino acids, the construction of possible loops, and the initial refinement of amino acid side chains.

Mutagenesis and Electrophysiology. HEK-293 cells (tsA201) were plated on glass coverslips and transfected with complementary DNA for wild-type and mutant *L. stagnalis* TASK (LyTASK) channels and green fluorescent protein for identification, as described previously.[8] Whole-cell recordings were made using an Axoclamp 200B amplifier (Axon Instruments, Foster City, CA). Pipets (3–5 MΩ) were fabricated from borosilicate glass. The intracellular solution contained (in mM) 120 KCH$_3$SO$_4$, 4 NaCl, 1 MgCl$_2$, 1 CaCl$_2$, 10 EGTA, 10 HEPES, 3 MgATP, and 0.3 NaGTP, titrated to pH 7.3 with KOH, and the extracellular solution contained (in mM) 145 NaCl, 2.5 KCl, 1 CaCl$_2$, 2 MgCl$_2$, 10 HEPES, and 10 D-glucose, titrated to pH 7.4 with NaOH. Solutions containing halothane were prepared from saturated solutions containing extracellular saline, as described previously.[36] Cells were voltage clamped at −80 mV, and voltage ramps from −120 to 0 mV and from 0 to −80 mV were performed over 250 ms. Currents were filtered at 100 Hz (−3 dB) using an 8-pole Bessel filter (model 900, Frequency Devices Inc., Ottawa, IL), digitized at 20 kHz (Digidata 1332A, Axon Instruments), and stored on a computer. Cells transfected with LyTASK channels exhibited outwardly rectifying currents, with reversal potentials typically ∼ −90 mV, close to the calculated potassium reversal potential of −98 mV. In order to quantify baseline LyTASK currents and the effect of halothane on LyTASK current, we measured the size of the current at the −50 mV point on the voltage ramp (see Figure 5A, vertical line, L = baseline current, H = halothane activated current). This holding potential was chosen to minimize any contribution from endogenous voltage-gated potassium currents (measurements on untransfected cells indicated that these endogenous voltage-gated currents were either minimal or not present). All experiments were carried out at 22

± 2 °C. Percentage activation was calculated from the ratio of the halothane activated current, H, and the control LyTask current, L, using the equation: activation = (H/L − 1) × 100%.

■ ASSOCIATED CONTENT

Ⓢ Supporting Information

Three-dimensional coordinates of the LyTASK model in PDB format. This material is available free of charge via the Internet at http://pubs.acs.org/.

■ AUTHOR INFORMATION

Corresponding Author

*E-mail: edwardb@stanford.edu.

Author Contributions

Bertaccini and Trudell performed the molecular modeling. Dickinson and Franks performed the in vitro mutations and electrophsyiology. All authors contributed to the approach to the work, as well as its analyses, interpretations, and actual manuscript composition.

■ REFERENCES

(1) Bayliss, D. A., and Barrett, P. Q. (2008) Emerging roles for two-pore-domain potassium channels and their potential therapeutic impact. *Trends Pharmacol. Sci. 29*, 566−575.

(2) Franks, N. P., and Honore, E. (2004) The TREK K2P channels and their role in general anaesthesia and neuroprotection. *Trends Pharmacol. Sci. 25*, 601−608.

(3) Lesage, F., and Lazdunski, M. (2000) Molecular and functional properties of two-pore-domain potassium channels. *Am. J. Physiol.: Renal Physiol. 279*, F793−801.

(4) Heurteaux, C., Guy, N., Laigle, C., Blondeau, N., Duprat, F., Mazzuca, M., Lang-Lazdunski, L., Widmann, C., Zanzouri, M., Romey, G., and Lazdunski, M. (2004) TREK-1, a K+ channel involved in neuroprotection and general anesthesia. *EMBO J. 23*, 2684−2695.

(5) Linden, A. M., Aller, M. I., Leppa, E., Vekovischeva, O., Aitta-Aho, T., Veale, E. L., Mathie, A., Rosenberg, P., Wisden, W., and Korpi, E. R. (2006) The in vivo contributions of TASK-1-containing channels to the actions of inhalation anesthetics, the alpha(2) adrenergic sedative dexmedetomidine, and cannabinoid agonists. *J. Pharmacol. Exp. Ther. 317*, 615−626.

(6) Pang, D. S., Robledo, C. J., Carr, D. R., Gent, T. C., Vyssotski, A. L., Caley, A., Zecharia, A. Y., Wisden, W., Brickley, S. G., and Franks, N. P. (2009) An unexpected role for TASK-3 potassium channels in network oscillations with implications for sleep mechanisms and anesthetic action. *Proc. Natl. Acad. Sci. U. S. A. 106*, 17546−17551.

(7) Lazarenko, R. M., Willcox, S. C., Shu, S., Berg, A. P., Jevtovic-Todorovic, V., Talley, E. M., Chen, X., and Bayliss, D. A. (2010)

Motoneuronal TASK channels contribute to immobilizing effects of inhalational general anesthetics. *J. Neurosci. 30*, 7691−7704.

(8) Andres-Enguix, I., Caley, A., Yustos, R., Schumacher, M. A., Spanu, P. D., Dickinson, R., Maze, M., and Franks, N. P. (2007) Determinants of the anesthetic sensitivity of two-pore domain acid-sensitive potassium channels: Molecular cloning of an anesthetic-activated potassium channel from *Lymnaea stagnalis*. *J. Biol. Chem. 282*, 20977−20990.

(9) Gruss, M., Bushell, T. J., Bright, D. P., Lieb, W. R., Mathie, A., and Franks, N. P. (2004) Two-pore-domain K+ channels are a novel target for the anesthetic gases xenon, nitrous oxide, and cyclopropane. *Mol. Pharmacol. 65*, 443−452.

(10) Patel, A. J., Honoré, E., Lesage, F., Fink, M., Romey, G., and Lazdunski, M. (1999) Inhalational anesthetics activate two-pore-domain background K$^+$ channels. *Nat. Neurosci 2*, 422−426.

(11) Talley, E. M., and Bayliss, D. A. (2002) Modulation of TASK-1 (Kcnk3) and TASK-3 (Kcnk9) potassium channels: Volatile anesthetics and neurotransmitters share a molecular site of action. *J. Biol. Chem. 277*, 17733−17742.

(12) Conway, K. E., and Cotten, J. F. (2012) Covalent modification of a volatile anesthetic regulatory site activates TASK-3 (KCNK9) tandem-pore potassium channels. *Mol. Pharmacol. 81*, 393−400.

(13) Franks, N. P., and Lieb, W. R. (1988) Volatile general anaesthetics activate a novel neuronal K+ current. *Nature 333*, 662−664.

(14) Franks, N. P., and Lieb, W. R. (1991) An anaesthetic-activated potassium channel. *Alcohol Suppl. 1*, 197−202.

(15) Scharf, M. T., and Kelz, M. B. (2013) Sleep and Anesthesia Interactions: A Pharmacological Appraisal. *Curr. Anesthesiol. Rep. 3*, 1−9.

(16) Murphy, M., Bruno, M. A., Riedner, B. A., Boveroux, P., Noirhomme, Q., Landsness, E. C., Brichant, J. F., Phillips, C., Massimini, M., Laureys, S., Tononi, G., and Boly, M. (2011) Propofol anesthesia and sleep: A high-density EEG study. *Sleep 34*, 283−291A.

(17) Miller, A. N., and Long, S. B. (2012) Crystal structure of the human two-pore domain potassium channel K2P1. *Science 335*, 432−436.

(18) Brohawn, S. G., Campbell, E. B., and Mackinnon, R. (2013) Domain-swapped chain connectivity and gated membrane access in a Fab-mediated crystal of the human TRAAK K+ channel. *Proc. Natl. Acad. Sci. U. S. A. 110*, 2129−2134.

(19) Brohawn, S. G., del Marmol, J., and MacKinnon, R. (2012) Crystal structure of the human K2P TRAAK, a lipid- and mechano-sensitive K+ ion channel. *Science 335*, 436−441.

(20) Franks, N. P. (2006) Molecular targets underlying general anaesthesia. *Br. J. Pharmacol. 147* (Suppl 1), S72−81.

(21) Franks, N. P. (2008) General anaesthesia: from molecular targets to neuronal pathways of sleep and arousal. *Nat. Rev. Neurosci 9*, 370−386.

(22) Rudolph, U., and Antkowiak, B. (2004) Molecular and neuronal substrates for general anaesthetics. *Nat. Rev. Neurosci 5*, 709−720.

(23) Jurd, R., Arras, M., Lambert, S., Drexler, B., Siegwart, R., Crestani, F., Zaugg, M., Vogt, K. E., Ledermann, B., Antkowiak, B., and Rudolph, U. (2003) General anesthetic actions in vivo strongly attenuated by a point mutation in the GABA(A) receptor beta3 subunit. *Faseb J. 17*, 250−252.

(24) Bertaccini, E. J., Yoluk, O., Lindahl, E. R., and Trudell, J. R. (2013) Assessment of Homology Templates and the Anesthetic Binding Site within the GABA Receptor. *Anesthesiology 119* (5), 1087−1095.

(25) Murail, S., Howard, R. J., Broemstrup, T., Bertaccini, E. J., Harris, R. A., Trudell, J. R., and Lindahl, E. (2012) Molecular Mechanism for the Dual Alcohol Modulation of Cys-loop Receptors. *PLoS Comput. Biol. 8*, e1002710.

(26) Bertaccini, E. J., Trudell, J. R., and Franks, N. P. (2007) The common chemical motifs within anesthetic binding sites. *Anesth. Analg. 104*, 318−324.

(27) Franks, N. P., Jenkins, A., Conti, E., Lieb, W. R., and Brick, P. (1998) Structural basis for the inhibition of firefly luciferase by a general anesthetic. *Biophys. J. 75*, 2205−2211.

(28) Franks, N. P., and Lieb, W. R. (1984) Do general anaesthetics act by competitive binding to specific receptors? *Nature 310*, 599−601.

(29) Altschul, S. F., Madden, T. L., Schaffer, A. A., Zhang, J., Zhang, Z., Miller, W., and Lipman, D. J. (1997) Gapped BLAST and PSI-BLAST: A new generation of protein database search programs. *Nucleic Acids Res. 25*, 3389−3402.

(30) Berman, H. M., Westbrook, J., Feng, Z., Gilliland, G., Bhat, T. N., Weissig, H., Shindyalov, I. N., and Bourne, P. E. (2000) The Protein Data Bank. *Nucleic Acids Res. 28*, 235−242.

(31) Braberg, H., Webb, B. M., Tjioe, E., Pieper, U., Sali, A., and Madhusudhan, M. S. (2012) SALIGN: a web server for alignment of multiple protein sequences and structures. *Bioinformatics 28*, 2072−2073.

(32) Higgins, D. G., Thompson, J. D., and Gibson, T. J. (1996) Using CLUSTAL for multiple sequence alignments. *Methods Enzymol 266*, 383−402.

(33) Eswar, N., Eramian, D., Webb, B., Shen, M. Y., and Sali, A. (2008) Protein structure modeling with MODELLER. *Methods Mol. Biol. 426*, 145−159.

(34) Brooks, B. R., Brooks, C. L., 3rd, Mackerell, A. D., Jr., Nilsson, L., Petrella, R. J., Roux, B., Won, Y., Archontis, G., Bartels, C., Boresch, S., Caflisch, A., Caves, L., Cui, Q., Dinner, A. R., Feig, M., Fischer, S., Gao, J., Hodoscek, M., Im, W., Kuczera, K., Lazaridis, T., Ma, J., Ovchinnikov, V., Paci, E., Pastor, R. W., Post, C. B., Pu, J. Z., Schaefer, M., Tidor, B., Venable, R. M., Woodcock, H. L., Wu, X., Yang, W., York, D. M., and Karplus, M. (2009) CHARMM: the biomolecular simulation program. *J. Comput. Chem. 30*, 1545−1614.

(35) Hwang, M. J., Stockfish, T. P., and Hagler, A. T. (1994) Derivation of Class II force fields. 2. Derivation and characterization of a class II force field, CFF93, for the alkyl functional group and alkane molecules. *J. Am. Chem. Soc. 116*, 2515−2525.

(36) de Sousa, S. L., Dickinson, R., Lieb, W. R., and Franks, N. P. (2000) Contrasting synaptic actions of the inhalational general anesthetics isoflurane and xenon [see comments]. *Anesthesiology 92*, 1055−1066.